TTI/VTI anisotropy estimation by focusing analysis, Part II: application

Y. He*, J. Cai, W. Whiteside, Z. Li, M. Guo, B. Wang, J. Xie, K. Yoon, E. Nessler
TGS-Nopec Geophysical Company, 2500 CityWest Blvd. Suite 2000, Houston, TX 77042, USA

Summary

The workflow for the practical application of the automated focusing analysis in time domain is demonstrated by deriving the TTI anisotropy parameters, epsilon and delta, from the previous VTI work in a small portion of the MC Revival survey located in the Mississippi Canyon area. The improvements are achieved for focusing of the dip events, optimized fault plane position, and imaging for base of salt position.

Introduction

Prestack isotropic depth migration and velocity model building have become a routine part of processing in order to image complex structures. In order to improve the positioning accuracy and the image quality, seismic anisotropy needs to be accounted for.

The majority of works on anisotropic model building for depth migration have concentrated on anisotropic tomography to flatten common imaging gathers (CIG) (Zhou et al., 2003, Zhou et al., 2004; Yuan et al. 2006).

Delphi proposed the common focus-point approach for isotropic migration velocity analysis, (Berkhout 1997), which splits the migration velocity analysis into two steps. First the migration operator is determined from the seismic data, and then the operator is translated into a velocity-depth model. Recently they used a one-way traveltime common focusing operator to construct the two-way traveltime common focusing operator (Verschuur and Marhfoul, 2009).

We (Cai et al. 2009) propose to apply the focusing analysis for CIG to derive the VTI or TTI anisotropy parameters epsilon and delta. The technique works for both VSP and surface seismic data. In this paper, we provide more details on the practical applications of this methodology in generating TTI anisotropic models from both synthetic data and field data.

Methodology

Figure 1 summarizes the general workflow for model building using anisotropic depth migration combined with the focusing analysis technique. The initial models can either be existing isotropic or anisotropic models.
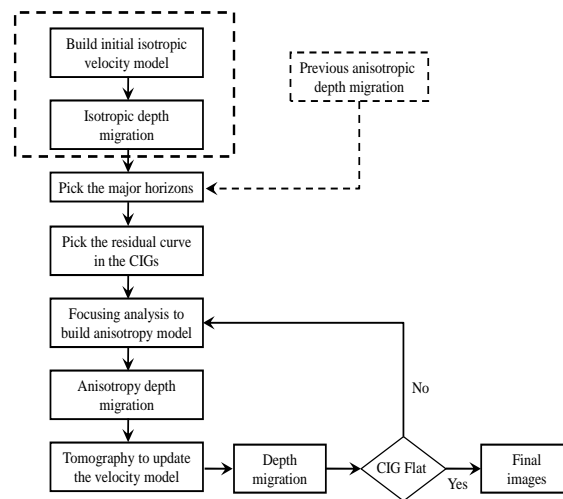

Figure 1: Anisotropy depth imaging workflow.

For anisotropic model building, the most challenge part is the coupling between the normal velocity and anisotropy parameters. For VTI media, we can build the initial vertical velocity model around the well location based on check shot information; implement isotropic depth migration; then derive the anisotropy parameters for those CIGs, which is similar to the workflow we proposed previously (Whiteside et al., 2008).

For TTI media, the most effective approach is to use VSP data to derive the anisotropic models. Figure 2 shows the focusing operators in time domain for a walk-away VSP derived from the BP 2008 TTI benchmark. After focusing analysis, the focusing operator moves from the magenta curve to the light blue curve, which is closer to the first arrival in the VSP. There are still some residuals left on the right branch, which means that further improvement of the anisotropy parameters will be needed. The magenta curve is almost overlapped by the light blue curve on the right side, which means the anisotropy symmetry axis should point to the top right (the green arrow); also the apexes of the curves are shifted. Both observations are consistent with our synthetic examples (Cai, et al. 2009). Figure 3 shows a comparison between the CIGs from surface seismic data derived VTI anisotropy models and from TTI walk-away VSP derived anisotropy models. We think that the focusing analysis was able to avoid the local minimums and converge to the global minimum.
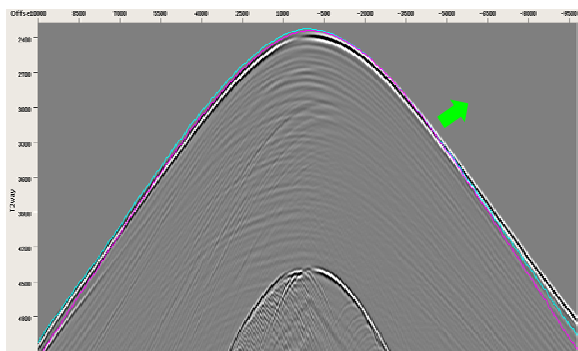
Figure 2: Focusing operators in time domain for walk-away VSP. The magenta is the focusing operator for isotropic media. The light blue is the focusing operator after update. (Data courtesy of BP)
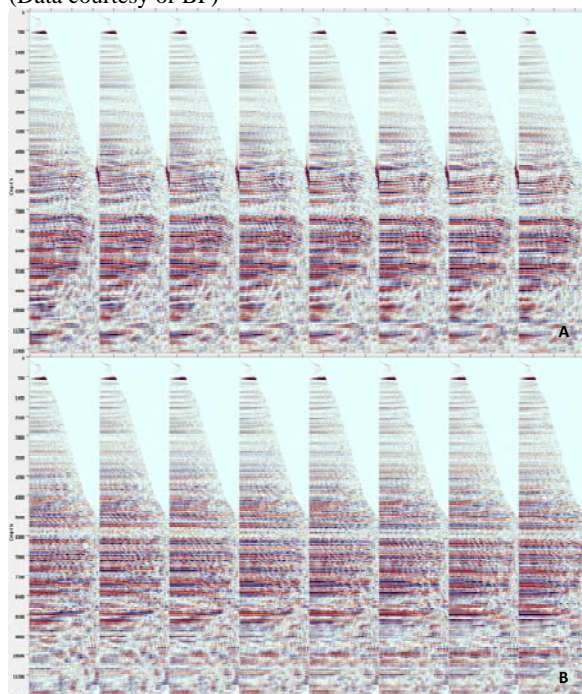

Figure 3: CIGs for the VTI anisotropy models derived from surface seismic data (A); and for the TTI anisotropy models derived from walk-away VSP focusing analysis (B). (Data courtesy of BP)

For the focusing analysis, the anisotropy model could be defined by either a grid based or a layer based model. Considering that normally the anisotropy follows the structure and the computation cost, our approach defines the anisotropy following the constant or gradient layers.

The field data that we studied is a small portion of the MC Revival survey. An high fidelity vertical velocity model for

VTI media was built with calibration to well information (Whiteside et al., 2008). Consider the factor that at the wells' locations within the selected area of the structure are relative flat. The VTI is a very good approximation for those locations. We take the final VTI vertical velocity model (Figure 4A) as initial normal velocity model for TTI anisotropy models. The VTI anisotropy parameters, epsilon and delta, are used to migrate a portion of the data within the study area to generate the initial VTI CIGs for focusing analysis. The TTI anisotropy symmetry axis angle is automatically calculated from the VTI migration stack section (Figure 4B).
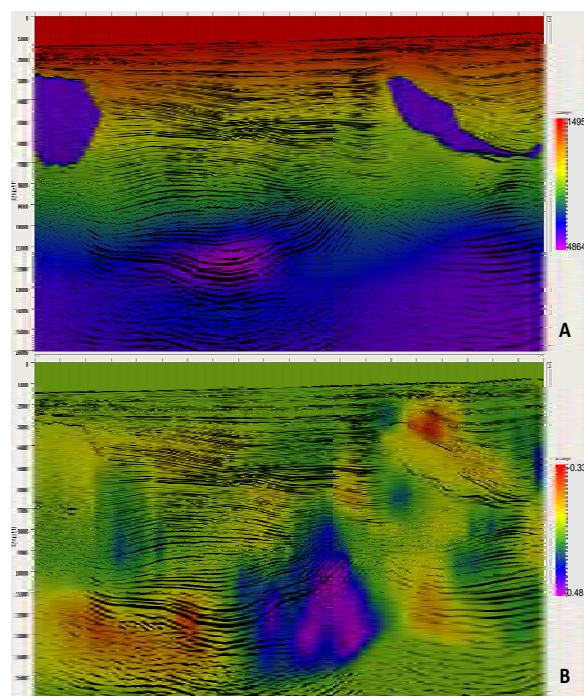

Figure 4: Inputs for focusing analysis. (A) Normal velocity model superimposed on VTI migration image. (B) TTI anisotropy symmetry axis angle superimposed on VTI migration image.

After pre-processing the CIGs and migrated stack, the focusing analysis program automatically picks the dominant events based on the CIGs around the well locations. The program then uses these picks as seeds from which to propagate outward in the migrated stack section (2D or 3D) in order to define the anisotropy layers for the CIGs (Figure 5).

Also based on the dominant events, the program picks the residual curvature for each CIG. There are couple options that user can choose to describe the residual curvature, such as simple parabolic curves, dual parameters curves

(Whiteside et al., 2008), and eta-curve equation (see the following equation) modified from the time-domain nonhyperbolic anisotropic NMO curve,

$$z^2(x) = z^2(x_0) + ax^2 - \frac{bx^4}{a\left[az^2(x_0) + (1+b)x^2\right]}$$

where x is the current offset, x_0 is the zero offset, z is depth for offset x, a and b are coefficients that determine the curvature. One advantage for dual parameters curve and eta-curve is that both of them yield depth variant curvatures for the same parameters/coefficients.
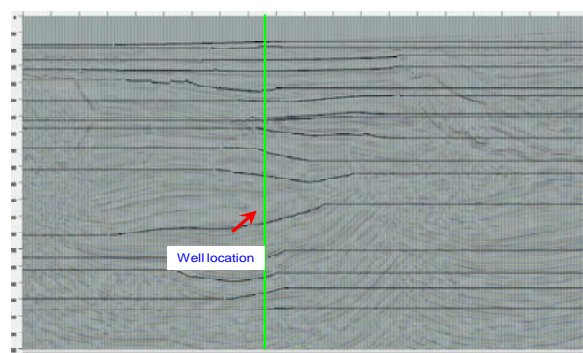

Figure 5: Automatically picked horizons around well.

Then the residual curvature, current normal velocity model, (for TTI) anisotropy symmetry axis angles, and anisotropy models are fed into the focusing analysis tool to derive the anisotropy models for this CIG location. The program allows the user respectively or simultaneously to search for epsilon and delta within a defined range. To avoid being trapped in a local minimum, we determined that searching for epsilon and delta simultaneously is a better option. Searching can be either exhaustive or non-linear inversion. Figure 6 shows the focusing analysis' object function for one of the events.

To build the 3D anisotropy model, we repeated the procedures stated above for those CIGs close to the wells with check shots; extrapolated the anisotropy parameters following the automatically or manually predefined anisotropy layers. Then we moved to the locations where the CIGs still have some residual moveout and fine tuned the anisotropy parameters at those locations. Finally we used 3D interpolation to build the anisotropy model. Figure 7 shows anisotropy models derived from the focusing analysis. Anisotropy models follow the structure pretty well. The epsilon and delta fields also have a degree of correlation.
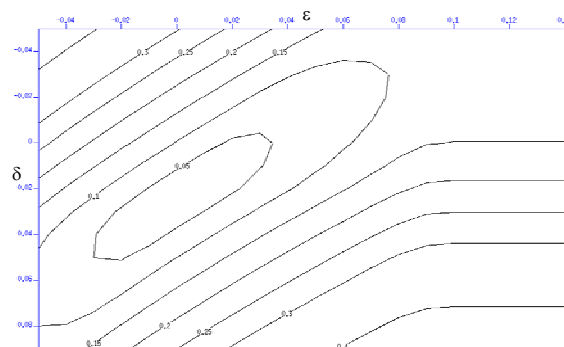

Figure 6: Objective function for focusing analysis from one of the events.
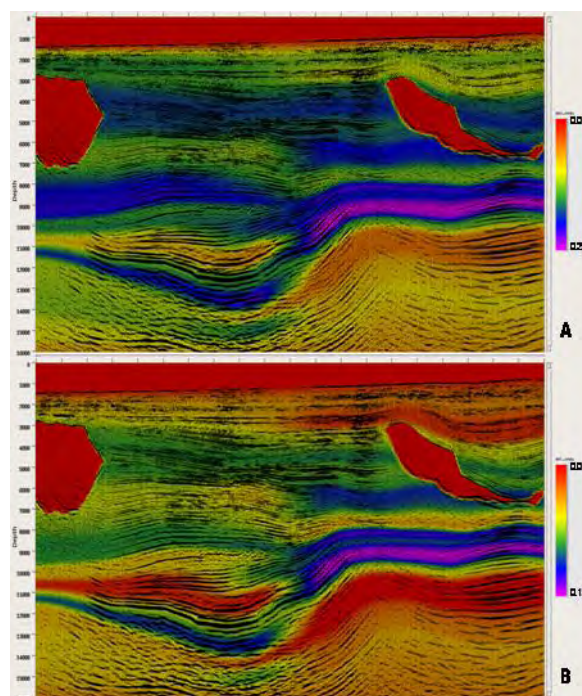

Figure 7: TTI anisotropy epsilon (A) and delta (B) models derived from focusing analysis.

Figure 8 shows the TTI migration using the anisotropy parameters derived by focusing analysis. Comparing between the VTI and TTI stack images (Figure 9), the dip layers become better focused (Figure 9A), the fault plane positions change slightly (Figure 9B), and the position of the base for the salt on the right is changed (Figure 9C). For Figure 9C, since focusing analysis was only used for the right side of the salt, the sediments above the salt on the that side are slight less focused.
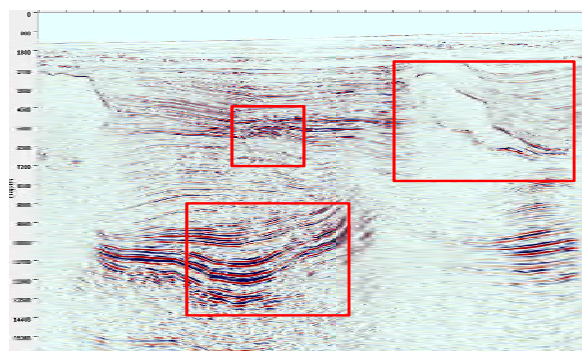
Figure 8: TTI migration imaging.

Conclusions

The focusing analysis technique was successfully applied to a small portion of MC Revival survey for TTI parameter estimation. The previous VTI vertical velocity model was used as the normal velocity model. The VTI epsilon and delta models were then used as initial models. The TTI anisotropy symmetry axis was calculated from the VTI stack section, and the VTI migrated CIGs were used as input CIGs for focusing analysis. The anisotropy models, epsilon and delta, derived from focusing analysis follow the structure fairly well. TTI migration improves the imaging for dip layers, fault plane positioning, and base of salt positioning.

Acknowledgments

The Authors would like to thank their colleagues Chuck Mason, Ashley Lundy, and Tefera Eshete for their valuable contributions during the project. We also thank BP for providing the TTI benchmark walk-away VSP and surface seismic data. And thanks to TGS-NOPEC for their support and the release of material for publication.
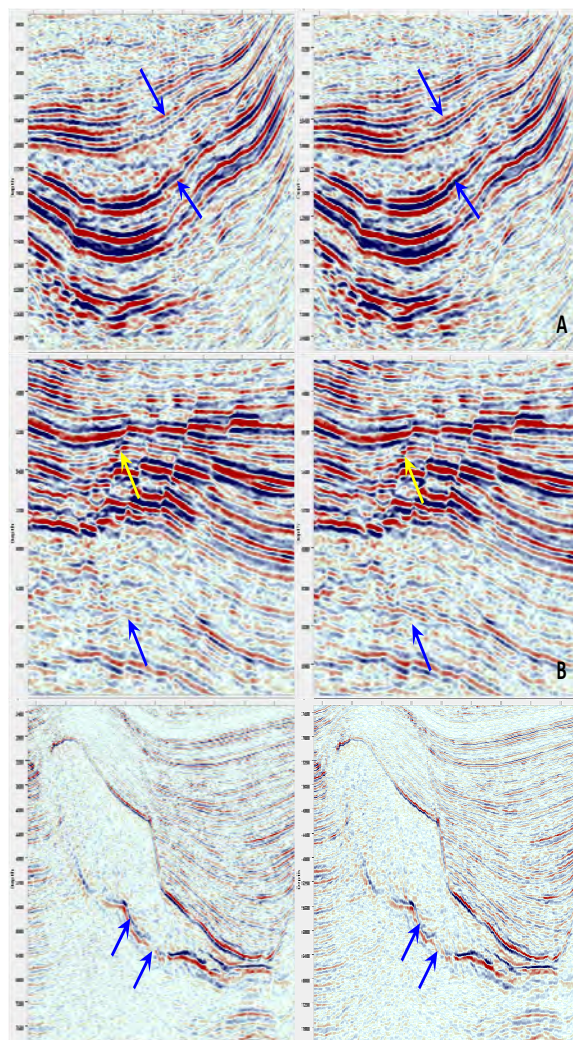

Figure 9: Zoom in comparison. Images on left are VTI migration images. Image on right are TTI migration images.

EDITED REFERENCES

Note: This reference list is a copy-edited version of the reference list submitted by the author. Reference lists for the 2009 SEG Technical Program Expanded Abstracts have been copy edited so that references provided with the online metadata for each paper will achieve a high degree of linking to cited sources that appear on the Web.

REFERENCES

Berkhout, A. J., 1997, Pushing the limits of seismic imaging, part II: integration of prestack migration, velocity estimation and AVO analysis: Geophysics, **62**, 954–969.

Cai, J., H. Yang, Z. Li, B. Wang, and M. Guo, 2009, TTI/VTI anisotropy estimation by focusing analysis, Part I: Theory: 79th Annual International Meeting, SEG, Expanded Abstracts, submitted.

Verschuur, E. and B. E. Marhfoul, 2009, Estimation of 2D and 3D near surface datuming operators by global optimization: DELPHI Acquisition and Preprocessing Project Volume XIII, Annual Report, Chapter 10.

Whiteside, W., W. Xu, Z. Li, A. Lundy, and I. Chang, 2008, Enhanced anisotropic model building methodology and pre-stack depth imaging in deep water gulf of Mexico: A case history, 78th Annual International Meeting, SEG, Expanded Abstracts, 358–362.

Yuan, J., X. Ma, S. Lin, and D. Lowrey, 2006, P-wave tomographic velocity updating in 3D inhomogeneous VTI media: 76th Annual International Meeting, SEG, Expanded Abstracts, 3368–3372.

Zhou, H., D. Pham, S. Gray, and B. Wang, 2003, 3-D tomographic velocity analysis in transversely isotropic media: 73th Annual International Meeting, SEG, Expanded Abstracts, 650–654.

Zhou, H., D. Pham, S. Gray, and B. Wang, 2004, Tomographic velocity analysis in strong anisotropic TTI media: 74th Annual International Meeting, SEG, Expanded Abstracts, 2347–2351.